Characterization of tyrosine ammonia lyases from Flavobacterium johnsonian and Herpetosiphon aurantiacus

Virklund, Alexander; Jendresen, Christian Bille; Nielsen, Alex Toftgaard; Woodley, John M

Published in:
Biotechnology Journal

Link to article, DOI:
10.1002/biot.202300111

Publication date:
2023

Document Version
Publisher's PDF, also known as Version of record

SHIMADZU
Excellence in Science

Higher Peaks – Clearly

Experience newfound clarity with the Nexera XS inert UHPLC. Offering reliable, robust performance, the Nexera XS inert represents a new peak in the analysis of biopolymers. It features a metal-free sample flow path prepared from corrosion-resistant materials, so that results will be clear and unaffected by sample adsorption or surface corrosion. Together with a new range of consumables, Shimadzu now offers the complete solution for bioanalysis.

Unconstrained recovery and sensitivity
Bioinert flow path prevents sample loss due to adsorption.

Clear resolution without restrictions
UHPLC performance for high efficiency bioanalysis.

Assured reliability and reproducibility
Corrosion-resistant material ensures long-term stability and reliable data acquisition.

Ultra High Performance
Liquid Chromatograph
Nexera XS inert

www.shimadzu.eu/higher-peaks

Received: 9 March 2023 | Revised: 12 June 2023 | Accepted: 12 July 2023

DOI: 10.1002/biot.202300111

Biotechnology Journal

RESEARCH ARTICLE

Characterization of tyrosine ammonia lyases from *Flavobacterium johnsonian* and *Herpetosiphon aurantiacus*

Alexander Virklund[1] | **Christian Bille Jendresen**[2] | **Alex Toftgaard Nielsen**[2,3] | **John M. Woodley**[1]

[1]Department of Chemical and Biochemical Engineering, Technical University of Denmark, Kgs Lyngby, Denmark

[2]Cysbio, Hørsholm, Denmark

[3]Novo Nordisk Foundation Center for Biosustainability, Technical University of Denmark, Kgs Lyngby, Denmark

Correspondence
John M. Woodley, Department of Chemical and Biochemical Engineering, Technical University of Denmark, 2800 Kgs Lyngby, Denmark.
Email: jw@kt.dtu.dk

Funding information
Novo Nordisk Foundation, Grant/Award Number: NNF17SA0031362

Abstract

p-Coumaric acid (*p*CA) can be produced via bioprocessing and is a promising chemical precursor to making organic thin film transistors. However, the required tyrosine ammonia lyase (TAL) enzyme generally has a low specific activity and suffers from competitive product inhibition. Here we characterized the purified TAL variants from *Flavobacterium johnsoniae* and *Herpetosiphon aurantiacus* in terms of their susceptibility to product inhibition and their activity and stability across pH and temperature via initial rate experiments. *Fj*TAL was found to be more active than previously described and to have a relatively weak affinity for *p*CA, but modeling revealed that product inhibition would still be problematic at industrially relevant product concentrations, due to the low solubility of the substrate tyrosine. The activity of both variants increased with temperature when tested up to 45°C, but *Ha*TAL1 was more stable at elevated temperature. *Fj*TAL is a promising biocatalyst for *p*CA production, but enzyme or bioprocess engineering are required to stabilize *Fj*TAL and reduce product inhibition.

KEYWORDS
biocatalysis, bioprocess engineering, modeling, protein stability

1 | INTRODUCTION

p-Coumaric acid (*p*CA) is a plant natural product with antioxidant and antimicrobial activity, and it is the precursor for a wide range of other phenylpropanoids including resveratrol and vanillin with potential uses in consumer food and health products. *p*CA can also be a precursor for 4-vinylphenol (4VP), which polymerizes to make the industrially relevant poly(4VP), which can be used to make organic thin film transistors. Unfortunately, the yields of *p*CA from plant extraction are low,[1] and it is costly to achieve high purities due to the presence of a wide variety of phenylpropanoids in plant biomass, which are difficult to separate. Bioprocessing is a promising alternative for *p*CA production which offers to produce high yields at high purity from renewable feedstocks such as sugars, glycerol from biodiesel production, or even CO_2.[2] The biological route for *p*CA production goes through the shikimic acid and aromatic amino acid pathways into phenylalanine or tyrosine, and then from phenylalanine to cinnamic acid to *p*CA, or directly from tyrosine to *p*CA (Figure 1).

The route typically found in plants that goes via phenylalanine may be less attractive for bioprocessing, because the oxidation of cinnamic acid requires a plant cytochrome P450 enzyme with poor soluble expression in bacterial expression hosts.[3] Additionally, the cytochrome P450 oxidation step requires co-factor regeneration, and is thus only feasible in metabolically active cells. The more direct route through tyrosine is easier to express in bacteria and does not require co-factors, but it has its' own limitations: The tyrosine ammonia

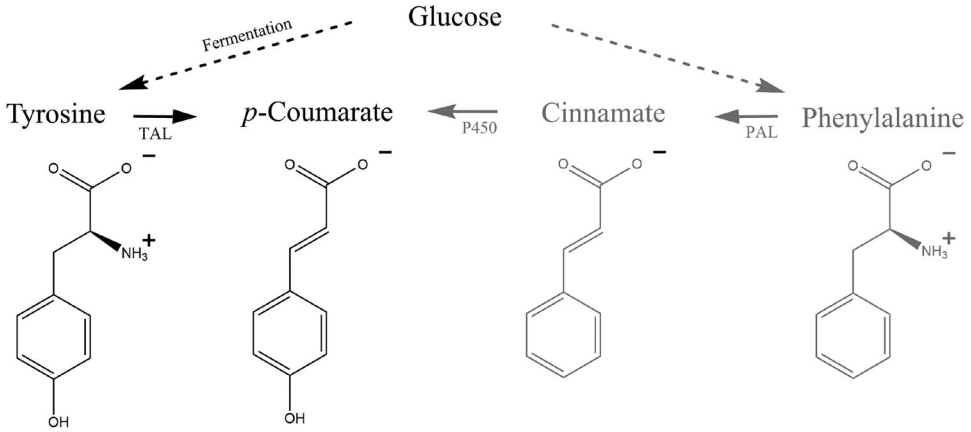

FIGURE 1 Biological routes for *p*CA production.

lyase (TAL) enzyme has a low specific activity and suffers from competitive product inhibition. Single-stage fermentations also suffer from low titers due to product toxicity that inhibits microbial growth. A two-stage bioprocess which decouples tyrosine fermentation in the first stage and enzymatic *p*CA production in the second stage was found to circumvent product toxicity and improve TAL specific activity.[4,5] Previously the yeast variants from *Rhodotorula glutinis* (*Rg*TAL) and *Phanerochaete chrysosporium* (*Pc*TAL) were tested in a two-stage bioprocess.[6] Since then, some promising bacterial variants from *Herpetosiphon aurantiacus* (*Ha*TAL1) and *Flavobacterium johnsoniae* (*Fj*TAL) were identified and characterized in terms of their pH profile and kinetic parameters, and found to be highly active and specific.[7] While these two bacterial variants have been evaluated and used for single-stage fermentation processes,[8,9] they have not been evaluated for their use in two-stage bioprocesses. Parameters of particular interest to a two-stage bioprocess include TAL activity at elevated temperatures, TAL stability, and the degree to which TAL is subject to product inhibition. Operating the enzymatic stage of the bioprocess at elevated temperature increases tyrosine solubility, and potentially increases TAL activity. TAL stability is required to enable biocatalyst recycling, which improves the economics of the process. Finally, TAL variants which are less subject to product inhibition may achieve higher activities in the presence of product inhibition. Here we characterize these properties of *Ha*TAL1 and *Fj*TAL, in addition to validating their pH profiles and kinetic parameters.

2 | EXPERIMENTAL SECTION

2.1 | Strain construction

Strains containing TAL plasmids were streaked on LB agar and grown overnight at 37°C.[7] A single colony of each strain was used to inoculate 3 mL LB media containing 50 mg/mL spectinomycin dihydrochloride pentahydrate (spec.) in 14 mL culture tubes, and incubated overnight at 37°C with shaking at 300 rpm and 25 mm. Plasmids were purified from the liquid cultures using QIAprep Spin Miniprep Kit (Qiagen) by following the manufacturer protocol.

Chemically competent cells of BL21(AI) were purchased from Invitrogen and transformed according to the TSS method with modifications:[10] Chemically competent cells were transformed with ~10–40 ng plasmid DNA, including a 30 s heat shock at 42°C before the addition of 950 µL SOC recovery media. Transformed cells were allowed to recover for 1 h at 37°C before plating and incubating overnight on chemically defined MDAG-11 plates without inducing activity,[11] except 25 mM $(NH_4)_2SO_4$ was used in place of 50 mM NH_4Cl and 5 mM Na_2SO_4, and 1.5% agar was used rather than 1% agar. 200 mg/L spec. was used in these plates, due to the antagonistic effect of phosphate against aminoglycosides.[12,13] The strains used in this study are listed in Table S1.

2.2 | Protein expression

Three single colonies of each expression strain were used to inoculate 500 µL MDAG-135 media[11] with 100 µL/mL spec. for an overnight preculture (~17 h) at 30°C with shaking at 210 rpm and 25 mm in 14 mL culture tubes, before being cooled to 4°C. All three colonies from each transformant were pre-screened for protein expression and found to be positive, and a single preculture for each strain was frozen as glycerol stocks at −80°C after mixing 750 µL culture with 750 µL 80% w/w glycerol. 20 µL of the overnight precultures were used to inoculate shake flasks with rich media; 1% tryptone, 0.5% yeast extract, 2 mM $MgSO_4$, 0.2x trace metals mixture (Teknova, #T1001), 0.2% glucose, 0.2% glycerol, 0.1% aspartate, 25 mM Na_2HPO_4, 25 mM KH_2PO_4, 25 mM NH_4SO_4, 100 mg/L spectinomycin, modified from.[11] After ~4.5 h cultivation at 37°C with shaking at 250 rpm and 25 mm, at which point the optical density at 600 nm (OD_{600}) reached ~4, the cultures were induced by adding IPTG (0.5 mM final) and arabinose (0.1% final). Cultures were induced overnight at room temperature (20 ± 2°C) to a final OD_{600} of ~16, before transferring the cultures to falcon tubes and harvesting the cells by centrifugation at 3800 *g* and 4°C for 10 min.

The supernatants were discarded, and the cell pellets were frozen at −17°C.

2.3 | Protein purification and characterization

Frozen cell pellets were resuspended by gently pipetting in 1 mL B-PER phosphate lysis buffer (Thermo Scientific) including 0.5 mg/mL lysozyme, 1X EDTA free HALT Protease Inhibitor Cocktail (Thermo Scientific), and 10 U/mL DNAse1 (Thermo Scientific). The tubes were incubated at room temperature for 20 min, diluted 1:1 in 1.5X concentrated equilibrium/wash buffer (75 mM $NaPO_4$, 75 mM glutamate, 75 mM arginine-HCl, 0.75 M NaCl, 15% v/v glycerol, 30 mM imidazole, ∼100 mM NaOH, pH 8.0), and the tubes were gently mixed. The crude lysate was centrifuged at 4000 *g* for 5 min at 4°C to remove major cell debris, transferred to a microcentrifuge tube, and finally centrifuged at 20000 *g* for 10 min at 4°C to pellet remaining cell debris.

Histidine-tagged TAL proteins were extracted via immobilized metal affinity chromatography (IMAC), following supplier protocols: The full volume of diluted lysate was loaded in 0.4 mL batches onto a 0.2 mL Ni^{++} HisPur Nickel Spin Column (Thermo Scientific) and washed thrice in 1X equilibrium/wash buffer. Samples were eluted thrice into a tube containing EDTA (5 mM final), with 200 µL of elution buffer (50 mM NaPO4, 50 mM glutamate, 50 mM arginine-HCl, 0.5 M NaCl, 10% glycerol, 250 mM imidazole, ∼66 mM NaOH, pH 8.0). Eluted protein samples were pooled, and buffer exchanged on a 2 mL Zeba spin desalting column 7K MWCO (Thermo Scientific) into a storage buffer (25 mM HEPES, 0.5 M NaCl, 10% glycerol, pH 7.0), aliquoted into PCR tubes, flash frozen in a dry ice ethanol slurry, and stored at −80°C.

Protein concentration was determined by using the Pierce 660 nm Protein Assay Reagent (Thermo Scientific) and a bovine serum albumin (BSA) (Thermo Scientific) standard curve. Protein samples were denatured and separated via SDS-page, using a XCell SureLock Mini-Cell (Invitrogen) and 4%–12% NuPage Bis-Tris Plus Mini Gels (Invitrogen). Gels were stained using SimplyBlue SafeStain (Invitrogen), photographed with GelDoc Go Gel Imaging System (BIO-RAD), and analyzed with Image Lab Software 6.1 (BIO-RAD).

2.4 | TAL activity assays

Activity assays were performed in 200 µL total volumes containing tyrosine, 50 mM CHES at pH 9, 9.5, and 10- or 50-mM CAPS at pH 10.5 and 11 adjusted with NaOH according to the reaction temperature. 1 mM tyrosine was used for measuring activity across pH and temperature. Data for the enzyme kinetic parameters were collected using 50 to 2000 µM tyrosine and 0 to 199 µM *p*CA, except 10 mM tyrosine was used for determining the inactivation coefficient. Samples without enzyme were included and used for blank-correction. Activity assays were initiated by the addition of 1 µg enzyme. pCA production was followed for 1 h in UV-transparent 96-well microplates (Corning) by measuring the absorbance spectrum (from 220–700 nm) using a SPECTROstar Nano (BMG Labtech) plate reader. 16 h time course experiments were performed with a 50 µL n-hexadecane overlay to prevent evaporation, because we were unable to identify a supplier of UV-vis microplate lids, and because lids would introduce condensation. *p*CA production rate was calculated via the slope of the absorbance over time at 325, 360, or 380, and divided by the extinction coefficient for *p*CA at the respective pH and wavelength, which in each case was measured experimentally (Figure S1). 325 nm was used for the majority of samples, 360 nm was used for determinking $K_{i,pCA}$, and 380 nm was used for determining K_{inact}. The longer wavelengths were used when measuring larger concentrations of *p*CA to stay within the linear range of the detector. It was validated that neither the presence of enzyme nor substrate interfered with the absorbance measurements (Figure S2). TAL activity is reported as *p*CA production in U(µmol *p*CA/min)/g TAL The kinetic models were fitted using the least squares method, and parameters reported with two standard deviations of uncertainty.

3 | RESULTS

3.1 | TAL production and purification

*p*CA can disrupt the cellular membrane of bacteria, but it can also bind to genomic DNA to inhibit cellular functions.[14] Due to the high toxicity of especially intracellular *p*CA toward *E. coli*, early induction or leaky expression of TAL will lead to plasmid loss and low yields.[4] We achieved high TAL yields by expressing the enzymes in a Bl21(AI) strain, where the T7 polymerase is controlled by the tightly repressed P_{BAD} promoter, and by inducing expression in the mid exponential phase at a lower temperature (Figure S3A). All enzyme variants were highly purified (Figure S3B), but with different yields that were directly related to the expression levels. Our first attempts to purify *Fj*TAL using a cobalt column were found to give much worse yields than a nickel column (Figure S4), even though the columns were far from saturated with his-tagged protein. The small amounts of protein eluted from cobalt columns were found to form cloudy precipitates upon storage, giving the impression of protein aggregation. In addition to using nickel columns, the addition of 50 mM glutamate and arginine during purification improved yields visibly (Figure S4), presumably due to their ability to prevent protein aggregation.[15–17]

1 mM Co^{2+} (around 0.05%) was previously shown to fully inactivate *Rg*PAL, while 1 mM Zn^{2+} decreased *Rg*PAL activity by around 70%.[18] On the other hand, storage of *Rg*PAL in 0.01% of Co^{2+} or Zn^{2+} was reported to increase *Rg*PAL stability,[19] suggesting that the inactivation is reversible or concentration-dependent. We added EDTA to chelate Zn^{2+} that had leaked off the column, and used a desalting column to remove the EDTA-Zn^{2+} complex. Cell lysis via bead milling was also found to reduce TAL activity in crude lysates of 3 out of 4 variants compared to chemoenzymatic lysis using detergent and lysozyme (Figure S5).

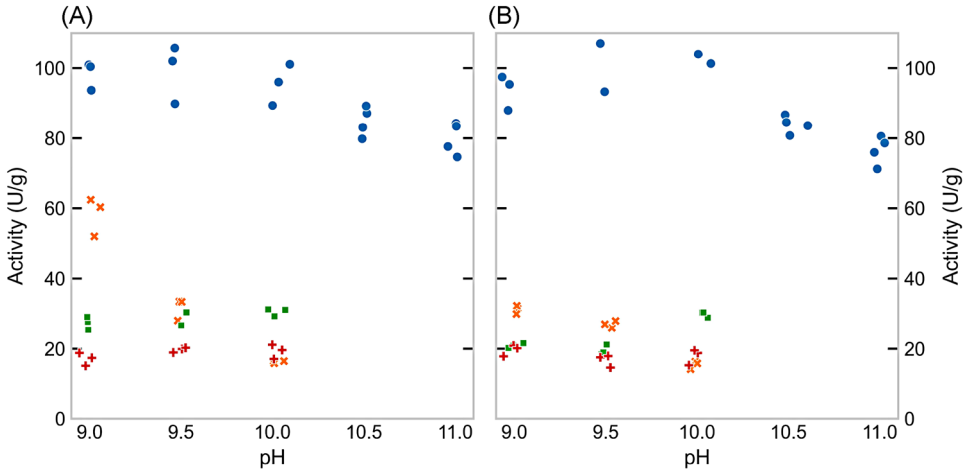

FIGURE 2 pH profiles of TAL variants in the absence (A) or presence (B) of 52 μM *p*CA. ■ *Rs*TAL; + SeSam8; **x** *Ha*TAL1; ● *Fj*TAL. Experiments were carried out at least in triplicate. Random jitter was added on the x-axis and does not imply variations in pH.

TABLE 1 Kinetic analysis of *Ha*TAL1 and *Fj*TAL.

TAL variant	pH	K_M (μM)	k_{cat} (s^{-1})	Study
*Ha*TAL1	9.5	48 ± 8	0.034 ± 0.008	This study
*Fj*TAL	9.5	33 ± 5	0.096 ± 0.002	This study
*Fj*TAL	9.5	152 ± 53 = $K_{i,pCA}$	-	This study
*Ha*TAL1	9	24	0.076	[7]
*Fj*TAL	9.5	6.7	0.023	[7]

3.2 | TAL activity across pH

Activity of the heterologously expressed and purified TAL proteins were measured in vitro in alkaline buffered solutions following the product formation by change in UV absorption (Figure 2A). We included TAL from *Rhodobacter sphaeroides* (*Rs*TAL) and *Saccharothrix espanaensis* (*Se*SAM8) in the initial comparisons, but these generally showed poor activities after purification, while *Ha*TAL1 and *Fj*TAL were more active. The measured activities across alkaline pH were in accordance with a previous characterization by Jendresen et al., except that purified *Fj*TAL was more than threefold as active in this case (Table 1). This increased activity may be due to differences in the expression and purification protocol, perhaps the use of a desalting column instead of overnight dialysis. *Fj*TAL activity was also measured at pH 11, where its' activity continued to decrease. Compared to the other TAL variants included here, *Fj*TAL is notable for its' high activity at and above pH 10, which may be useful for increasing tyrosine solubility. *p*CA is known to be a competitive inhibitor of TAL, and in the presence of 52 μM *p*CA *Rs*TAL and *Ha*TAL1 activities were drastically reduced (Figure 2B). Product inhibition of *Ha*TAL1 was less pronounced at pH 9.5 than at pH 9.0, and product inhibition of *Rs*TAL was less at pH 10, similar to what has been reported for other fungal TAL variants.[20] The activities of *Fj*TAL and *Se*Sam8 were not noticeably affected by 52 μM *p*CA regardless of pH.

3.3 | Kinetic characterization of *Ha*TAL1 and *Fj*TAL

While *Ha*TAL1 and *Fj*TAL had previously been characterized in terms of their K_M and k_{cat}, the activity of *Fj*TAL was much higher in the present study. We also wished to analyze the kinetic parameters of *Ha*TAL1 at pH 9.5 rather than 9 due to the weaker product inhibition at 9.5. Finally, because *Fj*TAL activity was not notably affected by 52 μM *p*CA, we wished to determine the K_i for *Fj*TAL in order to predict the impact of product inhibition at higher product concentrations. The initial rate of *Ha*TAL1 was measured across tyrosine concentrations (Figure S5), and the initial rate of *Fj*TAL was measured across tyrosine and *p*CA concentrations (Figure S6) to give the Michaelis Menten and competitive inhibition parameters (Table 1).

Just as the specific activity, the k_{cat} of *Fj*TAL was more than threefold higher than what was measured by Jendresen et al. Meanwhile, the V_{max} of *Ha*TAL1 was ~36% lower in this case and while the k_{cat} was less than half, it was measured at a different pH with lower V_{max}. In this case *Fj*TAL was found to be the most active of the four enzymes, which also matches the in vivo results with these enzymes.[7,23] The K_M values determined for *Ha*TAL1 and *Fj*TAL were higher than those determined by Jendresen et al.,[7] particularly for *Fj*TAL. The affinity of *Fj*TAL toward *p*CA (K_i = 152 μM) was found to be 4.6 times lower than the affinity toward tyrosine, which explains why the presence of 52 μM *p*CA did not noticeably decrease *Fj*TAL activity in a solution of 1 mM tyrosine. Conversely, while the K_i of *Ha*TAL1 was not determined here, the drastic decrease in activity in the presence of 52 μM *p*CA and 1 mM tyrosine suggests that *Ha*TAL1 has a higher affinity toward *p*CA than tyrosine at pH 9.

While the affinity of *Fj*TAL toward *p*CA is ~4.6 times lower than the affinity toward tyrosine, product inhibition is still relevant to consider for a batch biocatalytic process using *Fj*TAL. This is the case because of the low aqueous solubility of tyrosine, just ~10 mM at pH 9.5 and 25°C,[22,23] while *p*CA has a solubility of over 300 mM at the same pH and temperature. This is problematic, as the target

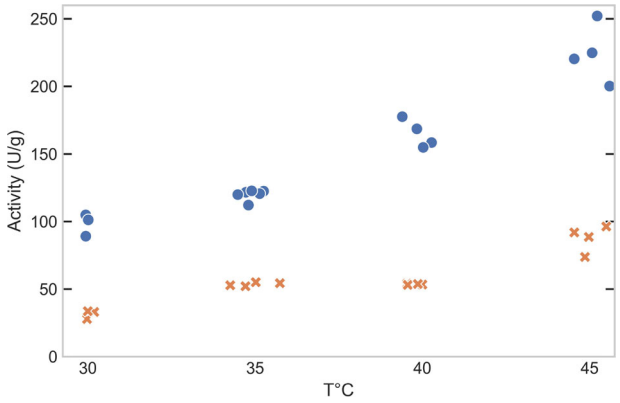

FIGURE 3 *Ha*TAL1 and *Fj*TAL activity across temperature at pH 9.5. x *Ha*TAL1; ● *Fj*TAL. Experiments were carried out at least in triplicate. Random jitter was added on the x-axis and does not imply variations in T.

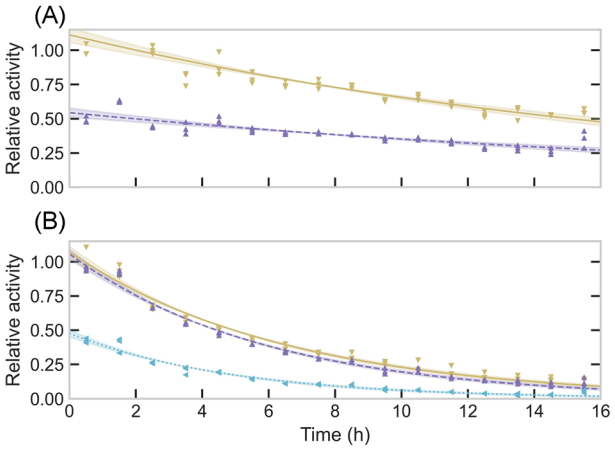

FIGURE 4 (A) *Ha*TAL1 activity over time at 45°C relative to mean *Ha*TAL1 activity at pH 9.5 0.5 h. (B) *Fj*TAL activity across time at 45°C relative to mean *Fj*TAL1 activity at pH 9.5 0.5 h. Derived from time course kinetic experiments and fitted to Equation (3). Experiments were carried out in triplicate. ▼—, pH 9.5; ▲---, pH 10; ◀……, pH 10.5.

titer for a *p*CA biocatalytic process is at a minimum 300 mM, so that the concentration of *p*CA in solution will be much higher than that of tyrosine throughout the majority of the process, and we predict the overall enzymatic rate will be greatly reduced. Product inhibition could be mitigated by increasing tyrosine solubility, which can be accomplished by increasing the pH and the temperature.[22–25] It was already shown that *Fj*TAL has relatively high activity up to pH 10.5 (Figure 2), where the solubility of tyrosine is around 50 mM at 25°C. Increasing the temperature 15°C increases the solubility of tyrosine in an unbuffered solution by approximately 63%,[25] and presumably there is a positive interaction between temperature and pH, given that the p*K*a values of tyrosine decrease with increasing temperature.[26]

3.4 | Temperature and TAL activity

Separate from tyrosine solubility, enzyme activity is also expected to increase with temperature, as long as the enzyme does not denature. To investigate this, the activities of *Ha*TAL1 and *Fj*TAL were measured from 30 to 45°C, and their activities were found to increase by 178% and 127% respectively by increasing the temperature 15°C (Figure 3).

3.5 | TAL stability

While *Ha*TAL1 and *Fj*TAL were shown to be active at 45°C pH 9.5, it was uncertain whether they would have long term stability under these conditions. Measuring the stability of *Ha*TAL1 and *Fj*TAL at pH 9.5 45°C with 0.5 M NaCl via a residual activity assay showed full stability for 6 h (Figure S8), which was unexpected based on preliminary time course experiments. To get a practical measurement of TAL stability we decided to do time course kinetic measurements on *p*CA production in the presence of tyrosine. Based on the kinetic parameters of *Fj*TAL, we could calculate that substrate depletion and product inhibition would be negligible at high substrate and low enzyme concentrations, which made it possible to estimate the inactivation coefficient k_{inact} as shown in Equation (3).

$$v\,(t) = \frac{k_{cat}\,[\mathrm{E}] * e^{-k_{inact} * t}\,\left([S] - [S]_t\right)}{[S] - [S]_t + K_m\left(1 + \frac{[P]_t}{K_i}\right)} \approx k_{cat}\,[\mathrm{E}] * e^{-k_{inact} * t} \qquad (3)$$

Since long-term incubation at 45°C would lead to evaporation and precipitation of tyrosine, we used an n-hexadecane organic overlay to prevent evaporation. Alkanes do not absorb light in the wavelengths of interest, and they have low affinity for tyrosine and *p*CA, which are hydrophilic at alkaline conditions. Incubating *Fj*TAL at room temperature with or without a hexadecane overlay yielded no differences in residual activity after 16 h (Figure S9). Also, the kinetic curves of *Fj*TAL and *Ha*TAL1 with tyrosine at 45°C were identical with and without the overlay for around 3 h, at which point precipitation and light scattering disrupted measurements without the overlay (Figure S10). Measuring *p*CA production for 16 h from pH 9.5 to 10.5 and deriving the activities over time yielded curves which fit Equation (3) well (Figure 4). The initial rate of *Fj*TAL at pH 10.5 relative to pH 9.5 was less than that which was found at 30°C (Figure 2), which suggests there may be a negative interaction between high pH and temperature in terms of *Fj*TAL activity. The activity of *Fj*TAL in all cases was reduced by approximately half after four hours, and less than 10% activity remained after 15.5 h. This indicates that it is impractical to recycle *Fj*TAL when used under these conditions.

The change in stability from pH 9.5 to 10 was insignificant for both variants, while the inactivation coefficient of *Fj*TAL increased slightly from pH 9.5 to 10.5 (Table S2). The stability of *Ha*TAL1 was around three times greater than that of *Fj*TAL despite a lower initial activity, so that the activity of *Ha*TAL1 after 15.5 h at pH 9.5 actually exceeded that of *Fj*TAL. Still, the amount of *p*CA accumulated after 16 h at pH 9.5 was approximately 40% higher for *Fj*TAL than *Ha*TAL1 (Table S2).

4 | DISCUSSION

4.1 | Kinetic characterization of TAL variants

The yield and activity of purified TAL enzymes was found to be highly dependent on the method of purification. This was the case when comparing *Fj*TAL activity to a previous study, as well as when comparing two different cell lysis methods in this study. The degree of product inhibition by *p*CA was found to be a major factor distinguishing TAL enzymes, which should be considered when comparing TAL variants for *p*CA production. In the case of a biocatalytic cascade toward derivative products, it is of course less relevant as *p*CA will not accumulate. The Michaelis constants were found to be similar for both *Ha*TAL1 and *Fj*TAL, and larger than what was previously reported for these enzymes. Low levels of *p*CA were found to inhibit *Ha*TAL1 and *Rs*TAL at pH 9 to a greater extent than at higher pH, similar to what was previously reported for *Rg*TAL.[24] *Fj*TAL was less impacted by product inhibition, and its' K_i was determined to be 152 μM, similar to what was recently reported for TAL from *Chryseobacterium luteum* sp. nov., and greater than the TALs from *Rivularia* sp. PCC 7116 and *Coprinopsis marcescibilis*.[31] Despite the higher affinity of *Fj*TAL toward tyrosine than *p*CA, we demonstrated that product inhibition is a major factor in reducing TAL activity in a potential batch biocatalytic process due to the low solubility of tyrosine. Engineering and selecting TAL variants with reduced affinity toward *p*CA compared to tyrosine (K_M /$K_{i,pCA}$ ratio) would alleviate product inhibition, but it is impractical to determine the affinity constants for many variants experimentally. Growth screens with phenylalanine or tyrosine as the sole carbon or nitrogen source have previously been used to select for ammonia lyases with higher K_{cat}, lower K_M, and reduced product inhibition.[31–33]

Increasing the solubility of tyrosine is another way to reduce product inhibition. The most dramatic increase is found when increasing pH, and a lesser increase is found when increasing temperature. The pH profiles of *Ha*TAL1 and *Fj*TAL were found to match those found previously,[7] with *Fj*TAL being fully active up to pH 10. The activities of both *Ha*TAL1 and *Fj*TAL were measured from 30 to 45°C and found to increase with increasing temperature in this range, in line with what was previously reported for other TAL variants.[20,30] The solubility of tyrosine has been shown to be greater in certain solvents such as ethyl acetate, dimethylformamide, dimethyl sulfoxide, and ethylene glycol than in water,[34,35] which could potentially be used as co-solvents. In practice these process parameters can only be increased as far as the enzyme allows without negatively affecting activity and stability.

4.2 | TAL stability

We found large disparities between the stability of both *Ha*TAL1 and *Fj*TAL measured via residual activity and time course kinetic assays, which bring into question the general practicality of enzyme stability data gathered via residual activity assays. *Ha*TAL1 was found to be almost threefold more stable at 45°C pH 9.5 than *Fj*TAL, the latter of which was relatively inactive after 15 h of catalytic activity. The cause of inactivation was not elucidated here, but it will be critical to improve the stability of *Fj*TAL in order to recycle the enzyme. Protein engineering may improve the stability of *Fj*TAL,[36] and clues into accomplishing this may be gained from studying the more stable *Ha*TAL1 or the thermostable *Pc*TAL. A growth screen as mentioned already,[31–33] could be modified to select for thermostability by using a thermophilic host and screening at higher temperatures. Other ways of improving TAL stability include using media additives and sparging with nitrogen,[28,37] or immobilizing the enzyme,[38] all of which could be considered for *Fj*TAL.

4.3 | Final thoughts

An alternative solution to reducing product inhibition is in-situ product removal,[39] although it may be difficult to find a suitable method in this case given the similarities between the substrate and product. Also, the plant route through phenylalanine may suffer less from product inhibition, because PAL is likely to have low affinity for *p*CA, and phenylalanine is much more soluble than tyrosine. *Fj*TAL is a promising enzyme candidate for a biocatalytic process producing *p*CA from tyrosine due to its' high activity at alkaline pH, at elevated temperatures, and in the presence of product inhibition, but a solution is needed to increase the stability of the enzyme in order for it to be industrially relevant.

Nomenclature

4VP	4-vinylphenol
k_{cat}	catalytic rate constant
K_i	inhibition constant
k_{inact}	inactivation rate constant
K_M	Michaelis constant
*p*CA,	*p*-Coumaric acid
[P]	product concentration
s	solubility
[S]	substrate concentration
spec.	spectinomycin dihydrochloride pentahydrate
t	time
T	temperature
v	enzyme activity

AUTHOR CONTRIBUTIONS

Alexander Virklund: Conceptualization, formal analysis, investigation, methodology, project administration, visualization, and writing – original draft. Alex Toftgaard Nielsen and John M. Woodley: Conceptualization, funding acquisition, supervision, and writing – review & editing. Christian Bille Jendresen: Material support, supevision, and writing - review & editing.

ACKNOWLEDGMENTS

This work was funded by the Novo Nordisk Foundation within the framework of the Fermentation-based Biomanufacturing Initiative (FBM), grant number: NNF17SA0031362.

CONFLICT OF INTEREST STATEMENT

Alexander Toftgaard Nielsen and Christian Bille Jendresen have ownership in Cysbio ApS, a company which holds a patent related to the production of *p*CA using *Fj*TAL and *Ha*TAL1.[40]

DATA AVAILABILITY STATEMENT

Data is available on request from the authors.

ORCID

Alexander Virklund https://orcid.org/0000-0003-4374-7641

REFERENCES

1. Timokhin, V. I., Regner, M., Hussain Motagamwala, A., Sener, C., Karlen, S. D., Dumesic, J. A., & Ralph, J. (2020). Production of p-Coumaric acid from Corn GVL-Lignin. *ACS Sustainable Chemistry & Engineering*, *8*, 17427–17438. https://doi.org/10.1021/acssuschemeng.0c05651
2. Gao, E. B., Kyere-Yeboah, K., Wu, J., & Qiu, H. (2021). *Photoautotrophic production of p-Coumaric acid using genetically engineered Synechocystis sp. Pasteur Culture Collection 6803*. Algal Research, 54. https://doi.org/10.1016/j.algal.2020.102180
3. Li, Y., Li, J., Qian, B., Cheng, L., Xu, S., & Wang, R. (2018). De Novo Biosynthesis of p-Coumaric Acid in *E. coli* with a trans-Cinnamic Acid 4-Hydroxylase from the Amaryllidaceae Plant Lycoris aurea. *Molecules (Basel, Switzerland)*, *23*(12), 3185. https://doi.org/10.3390/molecules23123185
4. Sariaslani, F. S. (2007). Development of a combined biological and chemical process for production of industrial aromatics from renewable resources. *Annual Review of Microbiology*, *61*(1), 51–69. https://doi.org/10.1146/annurev.micro.61.080706.093248
5. Ben-Bassat, A., Sariaslani, F., Huang, L., Patnaik, R., Lowe, D. (2005). *Methods for the preparation of para-hydroxycinnamic acid and cinnamic acid at alkaline PH* (DuPont US Holding LLC, U.S. 20050260724A1). Retrieved June 27, 2022, from https://patents.google.com/patent/US20050260724A1/en?oq=+U.S.+Patent+Appl.+2005260724%2C+2005
6. Huang, L. L., Xue, Z., & McCluskey, M. P. (2006). *Method of production of para-hydroxycinnamic acid using a thermostable TAL enzyme* (DuPont US Holding LLC, U.S.7572612B2).
7. Jendresen, C. B., Stahlhut, S. G., Li, M., Gaspar, P., Siedler, S., Förster, J., Maury, J., Borodina, I., & Nielsen, A. T. (2015). Highly active and specific tyrosine ammonia-lyases from diverse origins enable enhanced production of aromatic compounds in bacteria and Saccharomyces cerevisiae. *Applied and Environmental Microbiology*, *81*(13), 4458–4476. https://doi.org/10.1128/AEM.00405-15
8. Rodriguez, A., Kildegaard, K. R., Li, M., Borodina, I., & Nielsen, J. (2015). Establishment of a yeast platform strain for production of p-Coumaric acid through metabolic engineering of aromatic amino acid biosynthesis. *Metabolic Engineering*, *31*, 181–188. https://doi.org/10.1016/j.ymben.2015.08.003
9. Calero, P., Jensen, S. I., & Nielsen, A. T. (2016). Broad-host-range ProUSER vectors enable fast characterization of inducible promoters and optimization of p-Coumaric acid production in pseudomonas putida KT2440. *ACS Synthetic Biology*, *5*(7), 741–753. https://doi.org/10.1021/acssynbio.6b00081
10. Chung, C. T., Niemela, S. L., & Miller, R. H. (1989). One-step preparation of competent *Escherichia coli*: Transformation and storage of bacterial cells in the same solution (recombinant DNA). *Proceedings of the National Academy of Sciences*, *86*(7), 2172–2175.
11. Studier, F. W. (2018). T7 expression systems for inducible production of proteins from cloned genes in *E. coli*. *Current Protocols in Molecular Biology*, *124*(1). https://doi.org/10.1002/CPMB.63
12. Anderson, P. (1969). Sensitivity and resistance to spectinomycin in *Escherichia coli*. *Journal of Bacteriology*, *100*(2), 939–947. https://doi.org/10.1128/JB.100.2.939-947.1969
13. Studier, F. W. (2005). Protein production by auto-induction in high-density shaking cultures. *Protein Expression and Purification*, *41*(1), 207–234. https://doi.org/10.1016/j.pep.2005.01.016
14. Lou, Z., Wang, H., Rao, S., Sun, J., Ma, C., & Li, J. (2012). P-Coumaric acid kills bacteria through dual damage mechanisms. *Food Control*, *25*(2), 550–554. https://doi.org/10.1016/j.foodcont.2011.11.022
15. Golovanov, A. P., Hautbergue, G. M., Wilson, S. A., & Lian, L. Y. (2004). A simple method for improving protein solubility and long-term stability. *Journal of the American Chemical Society*, *126*(29), 8933–8939. https://doi.org/10.1021/JA049297H
16. Abe, R., Kudou, M., Tanaka, Y., Arakawa, T., & Tsumoto, K. (2009). Immobilized metal affinity chromatography in the presence of arginine. *Biochemical and Biophysical Research Communications*, *381*(3), 306–310. https://doi.org/10.1016/J.BBRC.2009.01.054
17. Shukla, D., & Trout, B. L. (2011). Understanding the synergistic effect of arginine and glutamic acid mixtures on protein solubility. *Journal of Physical Chemistry B*, *115*(41), 11831–11839. https://doi.org/10.1021/jp204462t
18. Zhu, L., Cui, W., Fang, Y., Liu, Y., Gao, X., & Zhou, Z. (2013). Cloning, expression and characterization of phenylalanine ammonia-lyase from *Rhodotorula glutinis*. *Biotechnology letters*, *35*(5), 751–756. https://doi.org/10.1007/S10529-013-1140-7/TABLES/2
19. Wall, M. J., Quinn, A. J., & D'Cunha, G. B. (2008). Manganese (Mn 2+)-dependent storage stabilization of *Rhodotorula glutinis* phenylalanine ammonia-lyase activity. *Journal of Agricultural and Food Chemistry*, *56*(3), 894–902. https://doi.org/10.1021/JF072614U
20. Xue, Z., McCluskey, M., Cantera, K., Ben-Bassat, A., Sariaslani, F. S., & Huang, L. (2007). Improved production of p-hydroxycinnamic acid from tyrosine using a novel thermostable phenylalanine/tyrosine ammonia lyase enzyme. *Enzyme and Microbial Technology*, *42*(1), 58–64.
21. Sáez-Sáez, J., Wang, G., Marella, E. R., Sudarsan, S., Cernuda Pastor, M., & Borodina, I. (2020). Engineering the oleaginous yeast Yarrowia lipolytica for high-level resveratrol production. *Metabolic Engineering*, *62*, 51–61. https://doi.org/10.1016/j.ymben.2020.08.009
22. Hitchcock, D. I. (1924). The solubility of tyrosine in acid and in alkali. *Journal of General Physiology*, *6*(6), 747–757. https://doi.org/10.1085/jgp.6.6.747
23. Lee, C. Y., Chen, J. T., Chang, W. T., & Shiah, I. M. (2013). Effect of pH on the solubilities of divalent and trivalent amino acids in water at 298.15K. *Fluid Phase Equilibria*, *343*, 30–35. https://doi.org/10.1016/J.FLUID.2013.01.010
24. Dunn, M. S., Ross, F. J., & Read, L. S. (1933). The solubility of the amino acids in water. *Journal of Biological Chemistry*, *103*(2), 579–595. https://doi.org/10.1016/s0021-9258(18)75836-5
25. Samuel, H., Yalkowsky, Y., & He, P. J. (2006). *Handbook of aqueous solubility data*. (2nd ed.). (Vol. 1999, Issue December, p. 9).
26. Nagai, H., Kuwabara, K., & Carta, G. (2008). Temperature dependence of the dissociation constants of several amino acids. *Journal of Chemical and Engineering Data*, *53*(3), 619–627. https://doi.org/10.1021/je700067a
27. Calabrese, J. C., Jordan, D. B., Boodhoo, A., Sariaslani, S., & Vannelli, T. (2004). Crystal structure of phenylalanine ammonia lyase: Multiple helix dipoles implicated in catalysis. *Biochemistry*, *43*(36), 11403–11416. https://doi.org/10.1021/bi049053+
28. El-Batal, A. I. (2002). Optimization of reaction conditions and stabilization of phenylalanine ammonia lyase-containing *Rhodotorula glutinis*

cells during bioconversion of trans-cinnamic acid to L-phenylalanine. *Acta Microbiologica Polonica*, *51*(2), 139–152.
29. CHMP. (2019). Committee for Medicinal Products for Human Use (CHMP) Assessment report. www.ema.europa.eu/contact
30. Brack, Y., Sun, C., Yi, D., & Bornscheuer, U. T. (2022). Discovery of novel tyrosine ammonia lyases for the enzymatic synthesis of p-Coumaric Acid. *Chembiochem*, *23*(10), e202200062. https://doi.org/10.1002/CBIC.202200062
31. McGuire, J. C., Montgomery, J. P., & Yang, H.-H. (1983). *Phenylalanine ammonia lyase-producing microbial cells* (Genex Corp., U.S. 4636466A). https://patents.google.com/patent/US4636466A/en?oq=US4636466
32. Mays, Z. J. S., Mohan, K., Trivedi, V. D., Chappell, T. C., & Nair, N. U. (2020). Directed evolution of Anabaena variabilis phenylalanine ammonia-lyase (PAL) identifies mutants with enhanced activities. *Chemical Communications*, *56*(39), 5255–5258. https://doi.org/10.1039/D0CC00783H
33. Trivedi, V. D., Chappell, T. C., Krishna, N. B., Shetty, A., Sigamani, G. G., Mohan, K., Ramesh, A., Pravin Kumar, R., & Nair, N. U. (2022). In-depth sequence-function characterization reveals multiple pathways to enhance enzymatic activity. *ACS Catalysis*, *12*(4), 2381–2396. https://doi.org/10.1021/ACSCATAL.1C05508/ASSET/IMAGES/MEDIUM/CS1C05508_M001.GIF
34. He, Q., Cong, Y., Zheng, M., Farajtabar, A., & Zhao, H. (2018). Solubility of l-tyrosine in aqueous solutions of methanol, ethanol, n-propanol and dimethyl sulfoxide: Experimental determination and preferential solvation analysis. *The Journal of Chemical Thermodynamics*, *124*, 123–132. https://doi.org/10.1016/J.JCT.2018.05.011
35. Li, X., Li, K., Farajtabar, A., He, Y., Chen, G., & Zhao, H. (2019). Solubility of d -Tryptophan and l -Tyrosine in several organic solvents: Determination and solvent effect. *Journal of Chemical and Engineering Data*, *64*(7), 3164–3169. https://doi.org/10.1021/acs.jced.9b00258
36. Hanson, A. D., McCarty, D. R., Henry, C. S., Xian, X., Joshi, J., Patterson, J. A., García-García, J. D., Fleischmann, S. D., Tivendale, N. D., & Harvey Millar, A. (2021). The number of catalytic cycles in an enzyme's lifetime and why it matters to metabolic engineering. *The Proceedings of the National Academy of Sciences USA*, *118*(13), e2023348118. https://doi.org/10.1073/pnas.2023348118
37. El-Batal, A. I. (2002). Continuous Production of L-Phenylalanine by *Rhodotorula glutinis* Immobilized cells using a column reactor. *Acta Microbiologica Polonica*, *51*(2), 153–169.
38. Wang, J., Zhang, N., Huang, Y., Li, S., & Zhang, G. (2022). Simple and efficient enzymatic procedure for p-Coumaric acid synthesis: Complete bioconversion and biocatalyst recycling under alkaline condition. *Biochemical Engineering Journal*, *188*, 108693. https://doi.org/10.1016/J.BEJ.2022.108693
39. Virklund, A., Jensen, S. I., Nielsen, A. T., & Woodley, J. M. (2022). Combining genetic engineering and bioprocess concepts for improved phenylpropanoid production. *Biotechnology and Bioengineering*, *120*(3), 613–628. https://doi.org/10.1002/BIT.28292
40. Gustav Stahlhut, S., Toftgaard Nielsen, A., & Kyst, R. (Cysbio ApS), U. S. 20200399665A1 (2020). Processes for the production of hydroxycinnamic acids using polypeptides having tyrosine ammonia lyase activity.

SUPPORTING INFORMATION

Additional supporting information can be found online in the Supporting Information section at the end of this article.

How to cite this article: Virklund, A., Jendresen, C. B., Nielsen, A. T., & Woodley, J. M. (2023). Characterization of tyrosine ammonia lyases from *Flavobacterium johnsonian* and *Herpetosiphon aurantiacus*. *Biotechnology Journal*, *18*, e2300111. https://doi.org/10.1002/biot.202300111